

## SIMULATION OF HEAT TRANSFER AND FLUID FLOW IN A POROUS BED OF IRON ORE PELLETS DURING UP- DRAUGHT DRYING

Anna-Lena LJUNG<sup>1</sup>, T. Staffan LUNDSTRÖM<sup>1</sup> and Kent TANO<sup>2</sup>

<sup>1</sup> Division of Fluid Mechanics, Luleå University of Technology, SE- 971 87, Luleå, Sweden

<sup>2</sup> LKAB, Research and Development, SE- 983 81, Malmberget, Sweden

### ABSTRACT

Iron ore pellets is one of the most refined products for companies such as LKAB and it is therefore a global need for research in the area in order to optimize the production and improve quality. This work aim at modelling and optimizing the drying zone of a travelling grate pelletizing plant and to start with, a model of velocity and temperature distribution in the up-draught drying zone is developed with aid of computational fluid dynamics. The velocity distribution in the porous bed is described by laws of fluid dynamics in porous media. The dominating heat transfer mechanism is convection and two energy equations are required since the porous media region contains both fluid and solid. Result from simulations show a rapid cooling of air due to the high specific surface area in the porous material. Conclusions are that it is possible to simulate convective heat transfer within a porous media in ANSYS CFX 10.0. There are however some limitations when using the diffusive transport equation as the solid phase energy equation that need further investigation. Moisture content and condensation in the bed are not included in the present model and is therefore subject to future work.

### NOMENCLATURE

$a_{sf}$  specific surface area of the packed bed [ $m^{-1}$ ]  
 $\alpha$  thermal diffusivity [ $m^2 s^{-1}$ ]  
 $A$  area perpendicular to flow direction [ $m^2$ ]  
 $c_p$  specific heat at constant pressure [ $J kg^{-1} K^{-1}$ ]  
 $D_p$  sphere particle diameter [ $m$ ]  
 $\varepsilon$  porosity  
 $h_{sf}$  convective heat transfer coefficient [ $W m^{-2} K^{-1}$ ]  
 $k$  thermal conductivity [ $W m^{-1} K^{-1}$ ]  
 $K$  permeability [ $m^2$ ]  
 $\rho$  density [ $kg m^{-3}$ ]  
 $p$  pressure [ $Pa$ ]  
 $Q$  volume flow [ $m^3 s^{-1}$ ]  
 $t$  time [ $s$ ]  
 $T$  temperature [ $^{\circ}C$ ]  
 $\mathbf{u}$  velocity [ $m s^{-1}$ ]  
 $U$  superficial fluid velocity [ $m s^{-1}$ ]  
 $\mu$  dynamic viscosity [ $kg m^{-1} s^{-1}$ ]

### Subscripts

$f$  fluid  
 $s$  solid

### INTRODUCTION

Before iron ores enter the blast furnace, it is necessary to remove a great portion of the mineral ballast components by graining. To remove these contaminations,

concentrates are very fine grained and agglomeration is therefore necessary. Agglomeration can be achieved by pelletizing and sintering. Ores containing large quantities of contaminations must be very fine-grained, and can therefore only be used for pellets. Due to advantages such as good transportability and mechanical strength, pellets are sometimes produced from good iron ore as well. Pellets are thus sintered spheres with high iron content. The average diameter for iron ore pellets is about 12 mm and 99 % of all pellets have a diameter in the range 6.3 - 16 mm and 70 % of these are, in their turn, within the interval 10-12.5 mm.

Pellets can be indurate in shaft furnaces, in grate-kilns and on travelling grates. The principle of sintering pellets is almost the same in grate-kilns and on travelling grates. The process starts with up- draught drying (UDD), followed by down- draught drying (DDD), a preheating zone, a burn zone and a cooling zone. The zone for burning is called firing on travelling grates and in great kiln for kiln. In the burning zone, magnetite is transformed to hematite through oxidation.

Before entering the drying zone, green balls are packed in a continuous bed. There are, as already mentioned, two possible flow directions for the drying air. Often a combination of these two types of drying are used, in order to make the lower layers more resistant to pressure. In UDD, hot air will make the lower part of the bed dry quickly but the air will soon cool from its inlet temperature to its evaporation temperature, which may lead to condensation in the upper part of the bed. The green balls are weakened when water condensate in the bed and this is one of the reasons why there is a limitation in bed height. When the green balls reach DDD, their strength has improved enough to avoid problems due to condensation. The heat supplied has to be controlled so that the moisture existing in the pores can escape through the capillaries without any over-pressure which would weaken the pellet structure. This phenomenon when over-pressure occurs is called chock drying and is one of the greatest limitations in inlet air temperature. Another reason to keep the temperature fairly low is the risk for early oxidation [1].

### THEORY

The governing equations for fluid flow are given as follows [2]:

Continuity equation

$$\frac{\partial \rho}{\partial t} + \nabla \cdot (\rho \mathbf{u}) = 0 \quad (1)$$

Momentum equation

$$\rho \frac{\partial \mathbf{u}}{\partial t} = -\nabla p + \mu \nabla^2 \mathbf{u} + \rho \mathbf{F} . \quad (2)$$

There are various forms of the momentum equation porous medium analogue to the Navier-Stokes equation. The commonly used Darcy's law is in refined and one dimensional form expressed as [3]

$$\frac{dp}{dx} = -\frac{\mu Q}{K A} . \quad (3)$$

The coefficient  $K$ , called permeability in single phase flow, is independent of the nature of the fluid and is exclusively given by the geometry of the medium. Darcy's law is valid as long as Reynolds number based on average grain diameter does not exceed some value, often between 1 and 10 [4]. As the velocity increases, the transition to nonlinear drag is quite smooth. This transition is to start with not from laminar to turbulent flow since at such comparatively small Reynolds number the flow in the pores is still laminar. The breakdown in linearity is rather due to increased inertia and is therefore a consequence of the tortuosity of the porespace. An equation that quite often fits data well over the entire range of Reynolds number is the Ergun equation [5]

$$\frac{\Delta p}{y} = 150 \frac{(1-\varepsilon)^2}{\varepsilon^3} \frac{\mu U}{D_p^2} + 1.75 \frac{(1-\varepsilon)}{\varepsilon^3} \frac{\rho U^2}{D_p} . \quad (4)$$

Regarding heat transfer, convection is the mode of energy transfer between a solid surface and the adjacent liquid or gas in motion and it involves the combined effects of conduction and fluid motion. Since motion of fluid is involved, heat transfer by convection is partially governed by the laws of fluid mechanics. Since the region with the porous media contains both fluid and solid, two energy equations are required. The energy equations can be presented in following form by taking averages over an elemental volume of the medium [6].

Fluid phase energy equation:

$$\varepsilon (\rho c_p)_f \frac{\partial T_f}{\partial t} + (\rho c_p)_f \mathbf{v} \cdot \nabla T_f = \nabla \cdot (\varepsilon k_f \nabla T_f) + a_{fs} h_{sf} (T_s - T_f) . \quad (5)$$

Solid phase energy equation:

$$(1-\varepsilon) (\rho c_p)_s \frac{\partial T_s}{\partial t} = \nabla \cdot ((1-\varepsilon) k_s \nabla T_s) + a_{sf} h_{sf} (T_f - T_s) . \quad (6)$$

The last terms in Eq. 5 and 6 have their origin in Newton's law of cooling. The convective heat transfer coefficient,  $h_{sf}$  is an experimentally determined parameter whose value depends on all variables influencing convection such as the surface geometry, the nature of fluid motion, the properties of the fluid and the bulk fluid velocities [7].

Specific surface area,  $a_{sf}$  is stated by the following expression which is developed from geometrical considerations [6]

$$a_{sf} = \frac{6(1-\varepsilon)}{D_p} . \quad (7)$$

## COMPUTATIONAL FLUID MECHANICS

CFX 10.0 uses the Finite Volume (FV) method as discretization approach. The solution domain is therefore subdivided into a finite number of contiguous control volumes (CV), and the conservation equations are applied to each CV.

Numerical solutions for fluid flow problems have various types of unavoidable errors, mainly modelling errors, discretization errors and iteration errors. Since the first one requires experiments to be determined in this case, focus is set on the latter errors [8].

Discretization error can be defined as the difference between the exact solution of the governing equations and the exact solution of the discrete approximation. Discretization errors can be estimated by retrieval of an extrapolated value when measurements from different grids are available [8].

Iteration error can be defined as the difference between the exact and the iterative solution of the discretized equations. The iteration error should be of an order of magnitude lower than discretization error. If the error level at the start of computation is known, the error will fall 2-3 orders of magnitude if the norm of residuals has fallen 3-4 orders of magnitude. This would imply that the first two or three most significant digits will not change in further iterations, and that the solution is accurate within 0.01-0.1 %.

The dimensionless parameter Courant number is one of the key parameters in transient CFD simulations and is defined as

$$c = \frac{u \Delta t}{\Delta x} \quad (8)$$

being the ratio of time step  $\Delta t$  to the characteristic convection time  $u/\Delta x$  that is the time required for a disturbance to be convected a distance  $\Delta x$ . When using explicit methods as transient schemes, the criterion to be satisfied is  $c < 1$ . Larger courant numbers are allowed when using the backward or implicit Euler method as transient scheme, but using too large values can lead to loss of numerical accuracy and each time step must have iterative convergence [8].

## MODELLING

The following assumptions are now introduced:

- Pellets are regarded as incompressible solid spheres with uniform diameter of 12 mm.
- The flow is assumed to be two dimensional with no regard taken to thermal- or mass flow from the bed surroundings. Effects due to movement of the bed are also neglected.
- Moisture content in the bed is not taken into account. Material parameters such as density and conductivity are based on sintered pellets

and are assigned constant values from Meyer [1] and earlier work at LKAB (See Appendix A).

- A bed of green balls is expected to have greater variation in porosity than a bed of fired pellets. Measurements of natural variation in packing of green balls are however not available and the variation is therefore estimated to be around 15% with a mean value of 0.41. The layer of fired pellets is approximately 0.1 m and is given a fix porosity of 0.39 which is an average porosity calculated from pellet density and bulk density.
- Since heat in a bed of pellets is up to 90% transferred by convection, all other heat transfer mechanisms will be left out of calculation.
- Only up- draught drying is investigated.
- The inlet air temperature is 300 °C and the initial temperature of the air and pellet in the bed is 35 °C in UDD.
- Thermal dissipation is not taken into account.

With these assumptions a porous domain is used to account for the porous material. When simulating heat transfer in porous media with ANSYS CFX 10.0, the fluid energy equation (Eq. 5) is automatically taken into account. However, a source term equal to the last term in Eq. 5 divided by  $\varepsilon$  must be added in order to solve for the convective heat transfer between solid and fluid.

The solid energy equation (Eq. 6) is not taken into account automatically, but may be included as a diffusive transport equation by the use of an additional variable. A source must be added here as well to account for the interaction between solid and fluid. Additional Variables (AV) are non-reacting, scalar components which are transported through the flow and ANSYS CFX 10.0 typically interprets additional variables as ‘concentrations’ within the fluid domain. In this case, the additional variable should provide a local average temperature in the solid material. The diffusive transport equation on specific form has the appearance

$$\frac{\partial(\varepsilon\rho_f\phi)}{\partial t} = \nabla \cdot (\varepsilon\rho_f\alpha\nabla\phi) + \varepsilon S \quad (9)$$

Since Eq. 9 is supposed to represent Eq. 6, the additional variable  $\Phi$  and the thermal diffusivity  $\alpha$  are stated as following:

$$\phi = \frac{T_{solid}(1-\varepsilon)\rho_s c_{ps}}{\varepsilon\rho_f} \quad (10)$$

$$\alpha = \frac{k_s}{\rho_s c_{ps}} \quad (11)$$

By substituting Eq. 10 and Eq. 11 with Eq. 9, the following transport equation is obtained:

$$\frac{\partial(1-n)\rho_s c_{ps} T_{solid}}{\partial t} = nS + \nabla \cdot \left( n\rho_f \frac{k_s}{\rho_s c_{ps}} \nabla \left( \frac{(1-n)\rho_s c_{ps} T_{solid}}{n\rho_f} \right) \right) \quad (12)$$

Eq. 12 implies some limitations in porosity and fluid density variations. Fluid density must be independent of temperature, pressure and location and the fluid used in calculations is therefore given constant material parameter values based on the mean temperature in the model. Porosity must, in the same way as density, have a constant value in the energy equations. It is however possible to let flow through the bed be a function of this variation in porosity, since the expressions of the linear and quadratic coefficients of Eq. 4 are specified in the porous loss model. Layers of different porosity due to differences in size and packing for green balls and fired pellets are implemented in the model with aid of step functions. To account for natural variation, randomly selected values of porosity within the interval 0.38-0.44 are interpolated over the whole region of green balls. A porosity value based on a volume average of the described variation is used in the energy equations.

A value of normal speed is applied at the inlet for stability reasons. The magnitude of the velocity is approximated from available process values of mass flows and velocities. The inlet superficial velocity is from this approximation given a value of 3.8 m/s. Since the value of velocity is based on a temperature of 300 °C, the velocity used as inlet boundary condition is recalculated with respect to density changes and set to 2.7 m/s. The outlet boundary condition is set to static pressure with zero as relative pressure. By taking the transfer coefficient as zero for the solid temperature inlet boundary condition, the only heat transfer between solid and fluid is done by the convective term in Eq. 5 and Eq. 6. Thermal energy is chosen as heat transfer model and gravity is neglected in the model.

The flow is assumed to be turbulent, based on the theory by Nield [3], since the pore Reynolds number for the conditions described above is  $\approx 3200$ . There are numerous turbulence models under investigation for flow in porous media. For example, Masuoka and Takatsu [9] proposed the 0- equation model, Antohe and Lage [10] a macroscopic turbulence  $k-\varepsilon$  model and Kuwahara *et al.* [11] performed a large eddy simulation (LES) study. Simulations in this work are carried out with a standard  $k-\varepsilon$  turbulence model with default intensity and length scale and automatic eddy dissipation since this model is expected to provide a good compromise in computational effort, robustness and accuracy. It is important to note that such a turbulence model only will take macroscopic turbulence effects into account and turbulence due to the porous matrix in a microscopic sense will be left out of calculations. Since only two dimensional flow effects are taken into account, the geometry of the bed is simplified in order to save computational time. By using a symmetry condition, only one half of the width of the geometry has to be included. Since the flow is assumed to be two dimensional, only one element in z- direction is used and symmetry conditions on the two boundaries are applied. A no slip boundary wall condition is imposed at the leaning wall. The bed height is 0.55 m and the top and bottom width of this bed is 3.654 m and 3.5 m, respectively. The simplified geometry together with boundary conditions is presented in Figure 1.

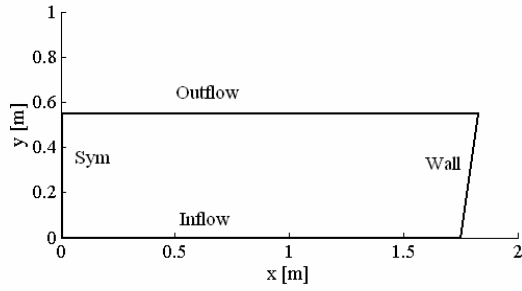


**Figure 1:** Simplified geometry with boundary conditions. Specified blend factor 1.0 is used as advection scheme and second order backward Euler as transient scheme.

## RESULT

A grid convergence test based on results from isothermal, steady state simulations with three consecutive grids is done in order to estimate the magnitude of the discretization error. Values of area average inlet pressure are used for the error analysis and the result is presented in Table 1. The RMS residual target is set to  $1e-7$  as convergence criteria, which in this case represents a reduction of iteration error with at least 2-3 orders of magnitude.

Grid No.	No. of nodes	Normalized number of nodes	Area average inlet pressure [Pa]
1	122042	1	5129.58
2	65520	1.86	5129.83
3	30940	3.94	5130.49

**Table 1:** Results from grid refinement study.

The results of the grid refinement study show monotone convergence. The polynomial curve in Figure 2 indicates that the results are in the asymptotic range and an extrapolated value of pressure for an infinitely fine mesh is thus obtained.

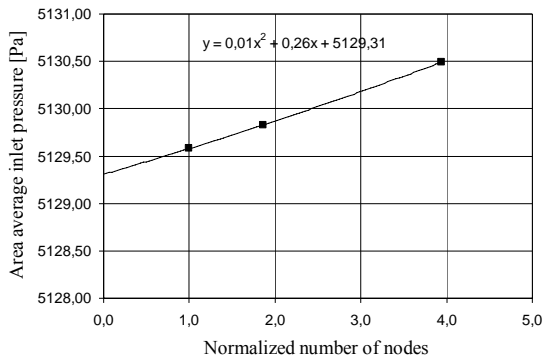


**Figure 2:** Area average inlet pressure as a function of normalized number of nodes. The extrapolated value and the corresponding estimated errors are shown in Table 2. The coarsest grid is used in all further simulations in order to save computational time.

$P_{extra}$ [Pa]	Error Grid 1 (%)	Error Grid 3 (%)
5129.31	0.0053	0.023

**Table 2:** Results from discretization error analysis.

The porosity distribution in the bed is presented in Figure 3. The natural variation of porosity is interpolated from ten randomly selected points and the corresponding flow distribution is presented in Figure 4.

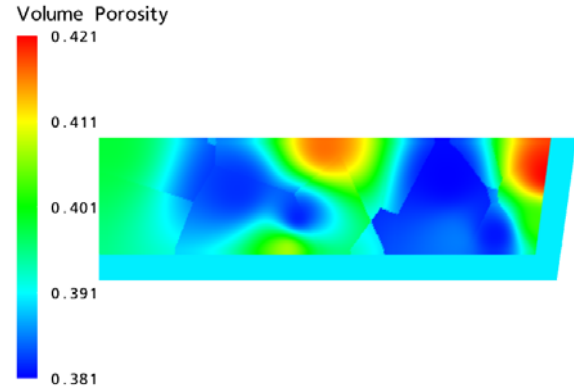


**Figure 3:** Porosity distribution.

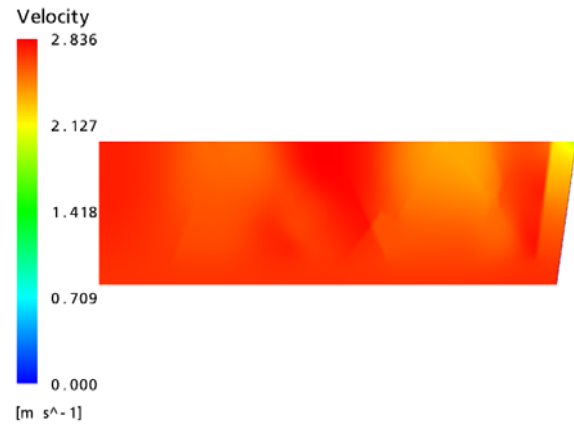


**Figure 4:** Velocity distribution.

For illustration of temperature distribution in fluid and solid, a transient simulation is carried out with iterative convergence criteria's fulfilled since a reduction of RMS residuals of at least three decades is achieved for every timestep. Evaluation of fluid temperature is illustrated in Figure 5 and the corresponding alteration in solid temperature in Figure 6. The graphs present temperature dependence on height for different time steps.

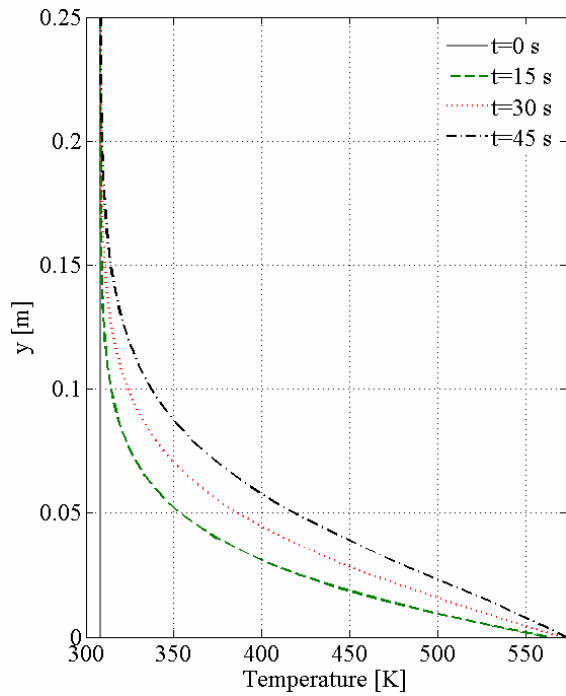


**Figure 5:** Fluid temperature distribution at  $x=0$  m presented at  $t=0$  s,  $t=15$  s,  $t=30$  s and  $t=45$  s.

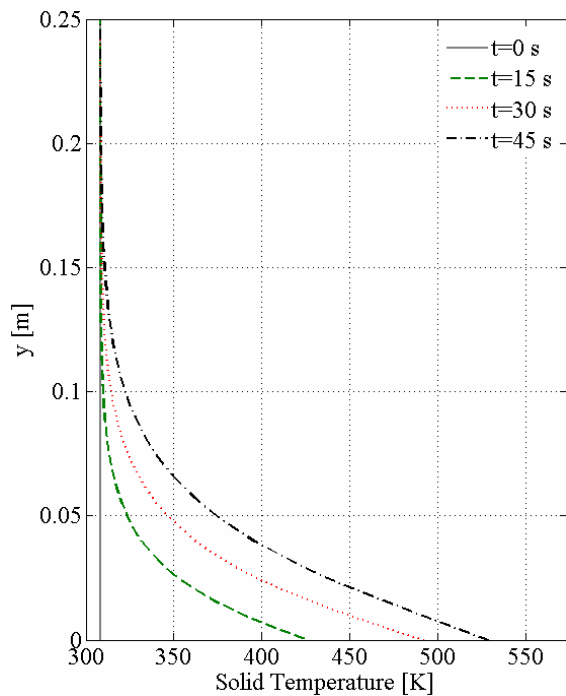


**Figure 6:** Solid temperature distribution at  $x=0$  m presented at  $t=0$  s,  $t=15$  s,  $t=30$  s and  $t=45$  s.

## DISCUSSION AND CONCLUSION

This work demonstrates the possibility of doing heat transfer models in ANSYS CFX 10.0 that calculates solid and fluid temperatures. Current limitations are limitations in density and porosity variation. The presented model show heat transfer tendencies, but to get a proper estimation of velocity and temperature distribution in the porous bed, further improvements are needed. It is also of

high importance to make validating experiments to compare with the simulation model in the future.

Flow effects due to movement of the bed and other influences from the process need to be further investigated as well as effects on heat transfer due to microscopic and macroscopic turbulence. In order to fully clarify drying of pellets, heat and moisture transport should also be investigated on a smaller scale since the present model does not take small scale effects into account.

Due to the complex porosity distribution in the bed, it is important to use appropriate approximations in order to make the permeability a function of both time and location. In this work, an investigation is made on how to implement such variations in CFX 10.0. It is however important to stress that the values used in the model are based on rough approximations and should not be considered otherwise. This work, however, facilitates further investigations on how to describe the bed in a proper way.

Both iteration errors and discretization errors should be negligible in comparison to modelling errors, since the assumptions in the model are arbitrary and convergence is achieved in all simulations.

## ACKNOWLEDGEMENTS

The authors express their gratitude to Magnus Malm, Simon Töyrä and Mats Strömsten at LKAB and Ulf Sjöström at MEFOS for valuable discussions and LKAB for financially backing up this work.

## REFERENCES

- [1] MEYER, K., "Pelletizing of iron ore", Springer-Verlag, Berlin, Heidelberg, 1980
- [2] KUNDU, PIJUSH K., COHEN, IRA M., "Fluid Mechanics", Academic Press, San Diego, 2<sup>nd</sup> ed., 2002
- [3] NIELD, DONALD A., BEJAN, ADRIAN, "Convection in Porous Media", Springer-Verlag, New York, 2<sup>nd</sup> ed., 1999
- [4] BEAR, JACOB, "Dynamics of Fluids in Porous Media", Dover publications Inc., New York, 1988
- [5] ERGUN, S., "Fluid flow through packed columns", Chemical Engineering Progress, Vol. 48, pp 89-94, 1952
- [6] AMIRI, A., VAFAI, K., "Analysis of dispersion effects and non-thermal equilibrium, non-Darcian, variable porosity incompressible flow through porous media", Int. J. Heat Mass Transfer, Vol. 37, No. 6, pp. 939-954, 1994
- [7] ÇENGEL, YUNUS A., "Introduction to thermodynamics and heat transfer", McGraw-Hill Inc., New York, 1997
- [8] FERZIGER, J.H., PERIĆ, M., "Computational Methods for Fluid Dynamics", Springer-Verlag, Berlin, 3<sup>rd</sup> ed., 2002
- [9] MASUOKA, T., TAKATSU, Y., "Turbulence model for flow through porous media", Int. J. Heat Mass Transfer, Vol. 39, No. 13, pp. 2803-2809, 1996
- [10] ANTOHE, B. V., LAGE, J. L., "A general two-equation macroscopic turbulence model for incompressible flow in porous media". Int. J. Heat Mass Transfer, Vol. 40, No. 13, pp. 3013-3024, 1997

- [11] KUWAHARA, F., YAMANE, T., NAKAYAMA, A.,  
 “Large eddy simulation of turbulent flow in porous  
 media”. International Communications in Heat and  
 Mass Transfer, Vol. 33, pp. 411-418, 2006

**APPENDIX A**

<b>Parameter</b>	<b>Value</b>	<b>Dimension</b>
Density	3700	$\text{Kg m}^{-3}$
Bulk density	2200	$\text{Kg m}^{-3}$
Convection heat transfer coefficients	190	$\text{W m}^{-2} \text{K}$
Average diameter	0.012	m
Porosity	0.39	
Specific heat capacity	560	$\text{J kg}^{-1} \text{K}^{-1}$
Thermal conductivity	0.4	$\text{W m}^{-1} \text{K}^{-1}$

**Table A.1:** Material parameters for fired pellets